



Temperature-Dependent Three-Dimensional Anisotropy of the Magnetoresistance in WTe₂

L. R. Thoutam,^{1,2} Y. L. Wang,^{1,*} Z. L. Xiao,^{1,2,†} S. Das,³ A. Luican-Mayer,³ R. Divan,³
 G. W. Crabtree,^{1,4} and W. K. Kwok¹

¹*Materials Science Division, Argonne National Laboratory, Argonne, Illinois 60439, USA*

²*Department of Physics, Northern Illinois University, DeKalb, Illinois 60115, USA*

³*Center for Nanoscale Materials, Argonne National Laboratory, Argonne, Illinois 60439, USA*

⁴*Departments of Physics, Electrical and Mechanical Engineering, University of Illinois at Chicago,
 Chicago, Illinois 60607, USA*

(Received 25 May 2015; published 22 July 2015)

Extremely large magnetoresistance (XMR) was recently discovered in WTe₂, triggering extensive research on this material regarding the XMR origin. Since WTe₂ is a layered compound with metal layers sandwiched between adjacent insulating chalcogenide layers, this material has been considered to be electronically two-dimensional (2D). Here we report two new findings on WTe₂: (1) WTe₂ is electronically 3D with a mass anisotropy as low as 2, as revealed by the 3D scaling behavior of the resistance $R(H, \theta) = R(\varepsilon_\theta H)$ with $\varepsilon_\theta = (\cos^2\theta + \gamma^{-2}\sin^2\theta)^{1/2}$, θ being the magnetic field angle with respect to the c axis of the crystal and γ being the mass anisotropy and (2) the mass anisotropy γ varies with temperature and follows the magnetoresistance behavior of the Fermi liquid state. Our results not only provide a general scaling approach for the anisotropic magnetoresistance but also are crucial for correctly understanding the electronic properties of WTe₂, including the origin of the remarkable “turn-on” behavior in the resistance versus temperature curve, which has been widely observed in many materials and assumed to be a metal-insulator transition.

DOI: 10.1103/PhysRevLett.115.046602

PACS numbers: 72.80.Ga, 71.18.+y, 75.47.Pq

Materials exhibiting large magnetoresistances, where their resistances change significantly with an applied magnetic field, are a key ingredient in modern electronic devices such as hard drives in computers [1]. The recent discovery [2] of extremely large magnetoresistances (XMRs) in WTe₂ has triggered extensive research to uncover the origin of XMRs in this material [2–12]. Since it is a layered compound with metal layers sandwiched between adjacent insulating chalcogenide layers, WTe₂ is typically considered to be electronically two dimensional (2D), whereby the anisotropic magnetoresistance is attributed only to the perpendicular component of the magnetic field $H \cos \theta$, where θ is the angle between the magnetic field H and the crystalline c axis [2,10]. A flatband lying below the Fermi surface is ascribed [3] to be the source of the remarkable transformative (“turn-on”) temperature behavior of the sample resistance, which first decreases with temperature and then increases rapidly at low temperatures [2]. Here, we show that WTe₂ is in fact electronically 3D with a small temperature-dependent anisotropy. The resistance follows a 3D scaling behavior [13] $R(H, \theta) = R(\varepsilon_\theta H)$ with $\varepsilon_\theta = (\cos^2\theta + \gamma^{-2}\sin^2\theta)^{1/2}$ with γ being the mass anisotropy, which varies from 1.9 to 5. Furthermore, we demonstrate the strong association of the anisotropy with the observed XMR where γ follows the monotonical increase of the magnetoresistance in the Fermi liquid state when the temperature is lowered.

We measured two samples that were cleaved out of bulk crystals purchased from HQ Graphene, Netherlands [14]. Their thicknesses are 190 nm (sample I) and 410 nm (sample II), respectively. Electric contacts with well-defined separations and locations were achieved using photolithography followed by evaporation deposition of a 300–500 nm thick Au layer with a 5 nm thick Ti adhesion layer. dc four-probe resistive measurements were carried out in a Quantum Design PPMS-9 using a constant current mode ($I = 100 \mu\text{A}$). An optic image of sample I is given as Fig. S1. Angular dependencies of the resistance were obtained by placing the sample on a precision, stepper-controlled rotator with an angular resolution of 0.05°. The magnetic field is always perpendicular to the current I which flows along the a axis of the crystal. More information on the relation of the a axis, the b axis, and the direction of current flow can be found in Fig. S1.

Figure 1 presents the typical magnetotransport behavior of a WTe₂ crystal (sample I) at $H \parallel c$. Figure 1(a) shows the temperature dependence of the resistance $R(T)$ of sample I. In the absence of a magnetic field, the resistance decreases monotonically with temperature, similar to those reported in the literature [2,4,8,10,12]. When an external magnetic field is applied along the c axis, the sample resistance increases and a remarkable turn-on behavior appears in the $R(T)$ curves at high magnetic fields ($H \geq 3$ T), where the temperature behavior of the resistance changes from

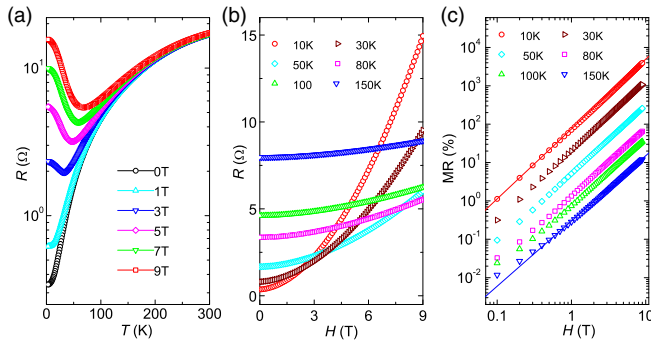


FIG. 1 (color online). Usual characterizations of sample I: (a) Resistance versus temperature $R(T)$ curves at various magnetic fields. (b) Resistance versus magnetic field $R(H)$ curves at various temperatures. (c) Magnetoconductance versus magnetic field curves $MR(H)$, in a log-log plot, demonstrating the power relationship, where the solid lines are fits of $MR \sim H^n$ with $n = 1.82$ at $T = 10$ K and $n = 1.7$ at $T = 150$ K. Data were taken with magnetic fields applied along the c axis of the crystal ($H \parallel c$), and we focus on the longitudinal resistance in this investigation.

metallic at high temperatures to “insulating” at low temperatures. The data also indicate that the amplitude of the magnetic-field-induced change in resistance increases with decreasing temperature and increasing magnetic field, consistent with the field dependence of the resistance $R(H)$ taken at various fixed temperatures presented in Fig. 1(b). The magnetoconductance, which is defined as $MR = [R(H) - R(0)]/R(0)$ and reported as a percentage, follows the typical power-law $MR \sim H^n$ behavior with n close to 2 as shown in Fig. 1(c).

In order to study the anisotropy of the resistance, we measured $R(H, \theta)$ at a fixed temperature. We chose a particular applied magnetic field angle θ with respect to the c axis of the crystal [see the inset of Fig. 2(c) for the definition of θ] and swept the magnetic field H to obtain $R(H)$. The data obtained for sample I at $T = 10$ and 125 K at various θ are presented in Figs. 2(a) and 2(b), respectively. They clearly reveal that the resistance is anisotropic, with larger resistance for a fixed magnetic field applied closer to the c axis ($\theta = 0^\circ$) for both temperatures. As discussed below in more detail, the data also indicate that the anisotropy associated with the change in resistance with θ is temperature dependent, i.e., larger at 10 K than that at 125 K.

Although the resistance anisotropy at $T = 10$ K presented in Fig. 2(a) is qualitatively consistent with those reported at low temperatures in the literature (inset of Fig. 3(b) in Ref. [2]), the pronounced magnetic field dependence of the resistance at $\theta = 90^\circ$ ($H \parallel b$ axis) ($MR = 320\%$ at 10 K and 9 T) contradicts the expectation of a 2D system in which only the perpendicular component $H \cos \theta$ should contribute to the magnetoconductance [2,10]; i.e., R should be independent of H at $\theta = 90^\circ$. On the other hand, as shown in Figs. 2(c) and 2(d), we found that the $R(H)$ curves obtained at a fixed temperature but at various

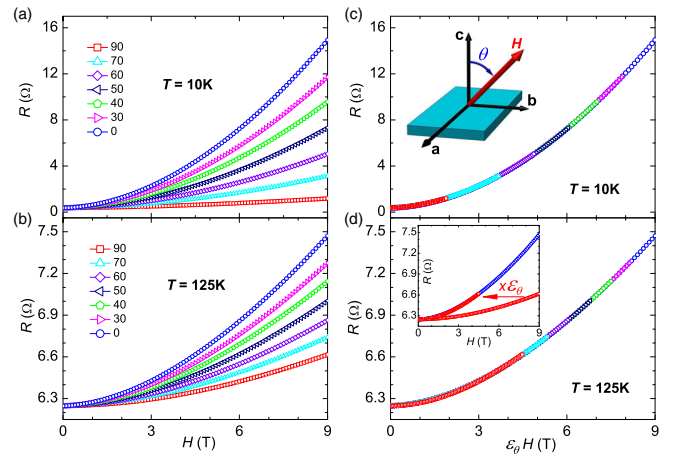


FIG. 2 (color online). Scaling behavior of the field dependence of the resistances obtained at various magnetic field orientations: (a),(b) $R(H)$ curves of sample I at various angles θ obtained at 10 and 125 K, respectively. (c),(d) Data in (a) and (b) replotted with H scaled by a factor ε_θ . The insets of (c) and (d) show the definition of angle θ (the current flows in the a - b plane along the a axis) and a schematic for the scaling operation (the data at 90° and 125 K were used as an example), respectively.

angles can be collapsed onto a single curve, $R(H, 0^\circ)$ data, with a field scaling factor $\varepsilon_\theta = (\cos^2 \theta + \gamma^{-2} \sin^2 \theta)^{1/2}$ where γ is a constant at a given temperature but changes from 4.762 at $T = 10$ K to 2.008 at $T = 125$ K. The temperature dependence of the scaling factor ε_θ for sample I and a second sample II is shown in Figs. 3(a) and 3(b), and illustrates the nice agreement with the experimental data. That is, the resistance of WTe_2 has the scaling behavior:

$$R(H, \theta) = R(\varepsilon_\theta H) \quad (1)$$

with $\varepsilon_\theta = (\cos^2 \theta + \gamma^{-2} \sin^2 \theta)^{1/2}$.

The above scaling behavior resembles that proposed for understanding the anisotropic properties of high temperature (high- T_c) superconductors [13]: the angle dependence of an anisotropic quantity $Q(H, \theta)$ has the scaling behavior $Q(H, \theta) = Q(\varepsilon_\theta H)$, where $\varepsilon_\theta H$ is the reduced magnetic field and $\varepsilon_\theta = (\cos^2 \theta + \gamma^{-2} \sin^2 \theta)^{1/2}$ reflects the mass anisotropy for an elliptical Fermi surface, with γ^2 being the ratio of the effective masses of electrons moving in directions of $\theta = 0^\circ$ and 90° . In the semiclassical model, the resistance R of a material is directly related to the mobility μ of the charge carriers through the relation $R = 1/ne\mu$ where $\mu = e\tau/m$, with m being the effective mass, τ the relaxation time, and e the electron charge. Thus, the anisotropy of the effective mass is expected to play a critical role in the anisotropic magnetoconductance. For example, using a two-band model, Noto and Tsuzuku [15] theoretically obtained the angle dependence of the magnetoconductance for graphite as $MR = A(\varepsilon_\theta H)^2 / [B + C(\varepsilon_\theta H)^2]$, where A , B , and C are constants and $\varepsilon_\theta = (\cos^2 \theta + \alpha \sin^2 \theta)^{1/2}$ with $\alpha = X^{-2}$ and $X = 12.1$ being the Fermi surface anisotropy k_z/k_x [15,16]. Since

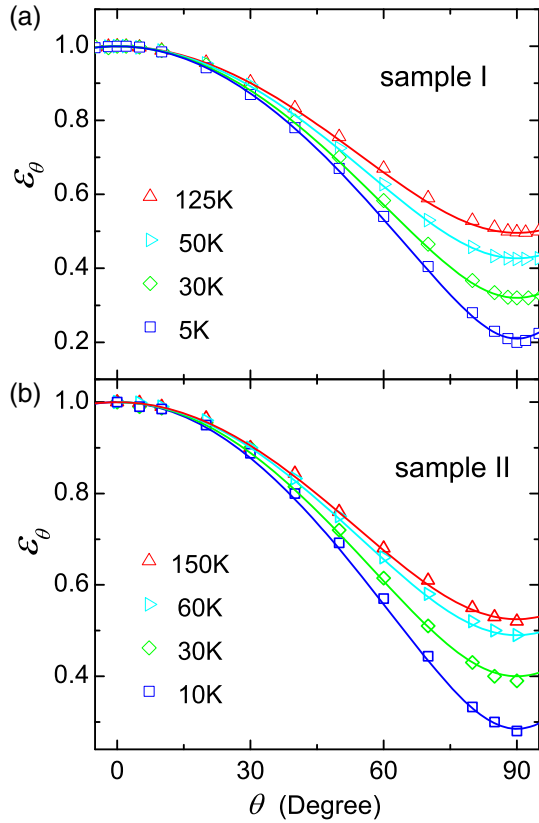


FIG. 3 (color online). Angle dependence of ε_θ at various temperatures for (a) sample I and (b) sample II. Symbols are derived from experimental data and lines are fits with $\varepsilon_\theta = (\cos^2 \theta + \gamma^{-2} \sin^2 \theta)^{1/2}$, where γ is a fitting parameter for a given temperature and the derived values at various temperatures for sample I are given in Fig. 4(a).

X can also be described as $X^2 = m_{\parallel}/m_{\perp}$, where m_{\parallel} and m_{\perp} are the effective masses parallel and perpendicular to the c axis [17], the theory developed to account for the angle dependence of the magnetoresistance in graphite is consistent with the general scaling rule for anisotropic superconductors and can be directly applied to understand the observed scaling behavior Eq. (1) for WTe_2 . That is, the value of γ obtained in our resistance scaling most likely reflects WTe_2 's Fermi surface anisotropy. As presented in Fig. 4(a), γ is close to 2 at high temperatures (>100 K), which is definitely much smaller than what one would naively expect for a 2D system [8]. It is even smaller than that (12.1) of graphite [15,16] and that (~ 8) of the well-known 3D high- T_c superconductor $\text{YBa}_2\text{Cu}_3\text{O}_7$ [18]. However, our results are consistent with the latest quantum oscillation experiments on WTe_2 , which reveal a 3D Fermi surface of moderate anisotropy [8]. The small anisotropy is probably due to the strong coupling caused by the distortion of the tellurium layers to accommodate the buckled zigzag tungsten chains [2,3].

A striking feature of the XMR in WTe_2 is the turn-on temperature behavior: in a fixed magnetic field above a

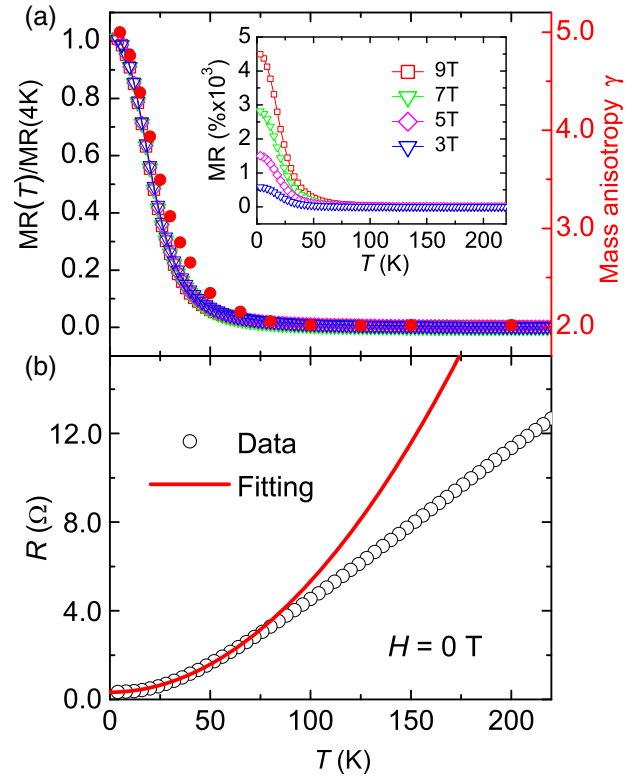


FIG. 4 (color online). Association of the anisotropy γ , XMR, and Fermi liquid state for sample I: (a) Temperature dependence of the MR (open symbols) and γ (red solid circles). (b) Temperature dependence of zero-field resistance (open circles). In (a), the original MR 's and the normalized values are given in the insets and in the main panels, respectively. In (b), symbols are the experimental data and the line represents a fit with the Fermi liquid model $R = \alpha + \beta T^2$.

certain critical value H_c , a turn-on temperature T^* is observed in the $R(T)$ curve, where it exhibits a minimum at a field-dependent temperature T^* . At $T < T^*$, the resistance increases rapidly with decreasing temperature while at $T > T^*$, it decreases with temperature [2]. This turn-on temperature behavior, which is also observed in many other XMR materials such as graphite [19,20], bismuth [20], PtSn_4 [21], PdCoO_2 [22], NbSb_2 [23], and NbP [24], is commonly attributed to a magnetic-field-driven metal-insulator transition and believed to be associated with the origin of the XMR [10,19,20,23,25]. Khveshchenko [25] predicted that at $T \leq T^*$ an excitonic gap Δ can be induced by a magnetic field in the linear spectrum of the Coulomb interacting quasiparticles with magnetic field dependence $\Delta(H \rightarrow H_c) \propto (H - H_c)^{1/2}$. However, the MRs obtained in our WTe_2 crystals at different magnetic fields as shown in Fig. 4(a) have the same temperature dependence, inconsistent with the existence of a magnetic-field-dependent gap, which should result in a steeper slope in the MR versus T curve at a higher field. Furthermore, we do not see any gap-opening-induced distinctive features such as steps at T^* in the MR

versus T curves in Fig. 4(a). Thus, the observed turn-on temperature behavior in WTe_2 is probably not due to a metal-insulator transition. In fact, thermopower experiments, which are capable of detecting a gap at the Fermi surface in the insulating state, also provide no evidence for the existence of an excitonic gap in graphite at low temperatures [26]. On the other hand, recent angle-resolved photoemission spectroscopy experiments have revealed that the Fermi surfaces of WTe_2 differ between 20 and 100 K, indicating that the observed XMR phenomenon in WTe_2 may be related to a change in the electronic structure with temperature.

Our second finding, presented in the main panel of Fig. 4(a) and Fig. S2a, is that the temperature dependence of γ , which is derived from the anisotropic magnetoresistance and probably directly related to the anisotropy of the Fermi surface, follows that of the MR 's: at low temperatures ($T < 75$ K), both MR and γ increase rapidly with decreasing temperature. At $T > 100$ K where MR is negligible, γ becomes small and virtually temperature independent. That is, the XMR in our WTe_2 crystals is probably linked to the electronic structure, more specifically, to the Fermi surface anisotropy, which can change with temperature due to the thermal expansion of the crystal and/or temperature-dependent electron-phonon coupling [3]. As presented in Fig. 4(b), the temperature dependence of the zero-field resistance of our WTe_2 crystals indeed shows a transition from linear behavior originating from the electron-phonon coupling at high temperatures to the $\alpha + \beta T^2$ behavior of a Fermi liquid state with dominant electron-electron scattering at low temperatures [27]. More important, the data in Fig. 4(a) also clearly show that γ starts to increase when the system enters the Fermi liquid state, enabling us to conclude that the XMR in WTe_2 occurs in the Fermi liquid state and its magnitude is positively correlated with the Fermi surface anisotropy. Similar results were obtained in sample II [28].

As evidently demonstrated in a wide range of superconductors, the mass anisotropy is the determining factor for the observed anisotropic properties [13,29]. Thus, we expect that Eq. (1) can be applicable in understanding the magnetoresistance anisotropy in other materials, which is often presented as $R(\theta)$ at a particular magnetic field value H ; i.e., the resistance is taken at a constant magnetic field while rotating the sample with respect to the external magnetic field. For example, the known Voigt-Thomson relation [15] $MR = M_1(H)\cos^2\theta + M_2(H)\sin^2\theta$ is a direct outcome of Eq. (1) if the magnetic field dependence of the resistance at $\theta = 0^\circ$ is quadratic. The $MR \sim (H \cos \theta)^{1.78}$ relation for graphite [30] is also approximated by Eq. (1) because at $\theta = 0^\circ$, $MR \sim H^{1.78}$ and the anisotropy $\gamma (\geq 12.1)$ is large [15,16]. In fact, Eq. (1) is the only versatile way to account for $R(\theta)$, since the MR 's magnetic field dependence at $\theta = 0^\circ$ varies from sample to sample or even changes with temperature for the same sample.

For example, the $MR(H)$ curves for most XMR materials follow a power-law relationship, but the exponent ranges from 1.6–2.5 [2,10,17,21,23,31]. In some cases, the $MR(H)$ cannot be described with a simple function [32]. As demonstrated in Fig. S3 for our sample [28], in which the $MR \sim H^n$ with temperature-dependent n , Eq. (1) can account for $R(\theta)$ curves obtained at different temperatures.

In summary, we find that WTe_2 is electronically 3D with a small mass anisotropy, which varies with temperature and follows the magnetoresistance behavior of the Fermi liquid state. These findings are crucial for correctly understanding the electronic properties, including the origin of the remarkable turn-on behavior in the resistance versus temperature curve, of WTe_2 and other XMR materials. We provide a general scaling approach for the anisotropic magnetoresistance, which is expected to account for the angle dependence of the magnetoresistance in many other systems, where various origins have been proposed and different fitting formulas have been applied.

This work was supported by DOE BES under Contract No. DE-AC02-06CH11357 which also funds Argonne's Center for Nanoscale Materials (CNM) and Electron Microscopy Center (EMC) where the nanopatterning and morphological analysis were performed. L. R. T. and Z. L. X. acknowledge NSF Grant No. DMR-1407175.

*ylwang@anl.gov

†xiao@anl.gov; zxiao@niu.edu

- [1] J. Daughton, *J. Magn. Magn. Mater.* **192**, 334 (1999).
- [2] M. N. Ali, J. Xiong, S. Flynn, J. Tao, Q. D. Gibson, L. M. Schoop, T. Liang, N. Haldolaarachchige, M. Hirschberger, N. P. Ong, and R. J. Cava, *Nature (London)* **514**, 205 (2014).
- [3] I. Pletikosić, M. N. Ali, A. V. Fedorov, R. J. Cava, and T. Valla, *Phys. Rev. Lett.* **113**, 216601 (2014).
- [4] W.-D. Kong, S.-F. Wu, P. Richard, C.-S. Lian, J.-T. Wang, C.-L. Yang, Y.-G. Shi, and H. Ding, *Appl. Phys. Lett.* **106**, 081906 (2015).
- [5] P. L. Cai, J. Hu, L. P. He, J. Pan, X. C. Hong, Z. Zhang, J. Zhang, J. Wei, Z. Q. Mao, and S. Y. Li, *arXiv:1412.8298v1*.
- [6] P. S. Alekseev, A. P. Dmitriev, I. V. Gornyi, V. Y. Kachorovskii, B. N. Narozhny, M. Schütt, and M. Titov, *Phys. Rev. Lett.* **114**, 156601 (2015).
- [7] J. Jiang, F. Tang, X. C. Pan, H. M. Liu, X. H. Niu, Y. X. Wang, D. F. Xu, H. F. Yang, B. P. Xie, F. Q. Song, X. G. Wan, and D. L. Feng, *arXiv:1503.01422v1*.
- [8] Z. Zhu, X. Lin, J. Liu, B. Fauqué, Q. Tao, C. Yang, Y. Shi, and K. Behnia, *Phys. Rev. Lett.* **114**, 176601 (2015).
- [9] X. C. Pan, X. Chen, H. Liu, Y. Feng, F. Song, X. Wan, Y. Zhou, Z. Chi, Z. Yang, B. Wang, Y. Zhang, and G. Wang, *arXiv:1501.07394v1*.
- [10] Y. Zhao, H. Liu, J. Yan, W. An, J. Liu, X. Zhang, H. Jiang, Q. Li, Y. Wang, X. Z. Li, D. Mandrus, X. C. Xie, M. Pan, and J. Wang, *arXiv:1502.04465v1*.
- [11] D. Kang, Y. Zhou, W. Yi, C. Yang, J. Guo, Y. Shi, S. Zhang, Z. Wang, C. Zhang, S. Jiang, A. Li, K. Yang, Q. Wu, G. Zhang, L. Sun, and Z. Zhao, *arXiv:1502.00493v2*.

- [12] F. X. Xiang, M. Veldhorst, S. X. Dou, and X. C. Wang, [arXiv:1504.01460v1](https://arxiv.org/abs/1504.01460v1).
- [13] G. Blatter, V. B. Geshkenbein, and A. I. Larkin, *Phys. Rev. Lett.* **68**, 875 (1992).
- [14] HQ Graphene, <http://www.hqgraphene.com>.
- [15] K. Noto and T. Tsuzuku, *Jpn. J. Appl. Phys.* **14**, 46 (1975).
- [16] D. E. Soule, *Phys. Rev.* **112**, 698 (1958).
- [17] D. E. Soule, J. W. McClure, and L. B. Smith, *Phys. Rev.* **134**, A453 (1964).
- [18] T. Ishida, K. Inoue, K. Okuda, H. Asaoka, Y. Kazumata, K. Noda, and H. Takei, *Physica (Amsterdam)* **263C**, 260 (1996).
- [19] X. Du, S.-W. Tsai, D. L. Maslov, and A. F. Hebard, *Phys. Rev. Lett.* **94**, 166601 (2005).
- [20] Y. Kopelevich, J. C. M. Pantoja, R. R. da Silva, and S. Moehlecke, *Phys. Rev. B* **73**, 165128 (2006).
- [21] E. Mun, H. Ko, G. J. Miller, G. D. Samolyuk, S. L. Bud'ko, and P. C. Canfield, *Phys. Rev. B* **85**, 035135 (2012).
- [22] H. Takatsu, J. J. Ishikawa, S. Yonezawa, H. Yoshino, T. Shishidou, T. Oguchi, K. Murata, and Y. Maeno, *Phys. Rev. Lett.* **111**, 056601 (2013).
- [23] K. Wang, D. Graf, L. Li, L. Wang, and C. Petrovic, *Sci. Rep.* **4**, 7328 (2014).
- [24] C. Shekhar, A. K. Nayak, Y. Sun, M. Schmidt, M. Nicklas, I. Leermakers, U. Zeitler, W. Schnelle, J. Grin, C. Felser, and B. Yan, [arXiv:1502.04361v1](https://arxiv.org/abs/1502.04361v1).
- [25] D. V. Khveshchenko, *Phys. Rev. Lett.* **87**, 206401 (2001).
- [26] T. Tokumoto, E. Jobiliong, E. Choi, Y. Oshima, and J. Brooks, *Solid State Commun.* **129**, 599 (2004).
- [27] H. D. Drew and U. Strom, *Phys. Rev. Lett.* **25**, 1755 (1970).
- [28] See Supplemental Material at <http://link.aps.org/supplemental/10.1103/PhysRevLett.115.046602> for an optic image of sample I and more data from sample II.
- [29] G. Blatter, M. V. Feigel'man, V. B. Geshkenbein, A. I. Larkin, and V. M. Vinokur, *Rev. Mod. Phys.* **66**, 1125 (1994).
- [30] K. Noto and T. Tsuzuku, *J. Phys. Soc. Jpn.* **35**, 1264 (1973).
- [31] T. Liang, Q. Gibson, M. N. Ali, M. Liu, R. J. Cava, and N. P. Ong, *Nat. Mater.* **14**, 280 (2015).
- [32] F. Y. Yang, K. Liu, K. Hong, D. H. Reich, P. C. Searson, C. L. Chien, Y. Leprince-Wang, K. Yu-Zhang, and K. Han, *Phys. Rev. B* **61**, 6631 (2000).